Configurations and level structure of ^{219}Rn

R. K. Sheline*
Departments of Chemistry and Physics, Florida State University, Tallahassee, Florida 32306

C. F. Liang and P. Paris
Centre de Spectrométrie Nucléaire et de Spectrométrie de Masse, Bâtiment 104, 91405 Campus Orsay, France

(Received 6 May 1997)

The level structure of ^{219}Rn has been studied using the alpha decay of ^{223}Ra and coincident gamma rays. While only modest changes are required in the level structure, and only above 342.8 keV, severe changes are required throughout the level scheme in the spin assigments. These changes allow the assignment of two sets of anomalous bands with $K=5/2^{\pm}$ and $K=3/2^{\pm}$. The $K=5/2^{\pm}$ bands have configurations intermediate between the reflection asymmetric configuration and the $g_{9/2}$ shell model configuration, while the $K=3/2^{\pm}$ bands have configurations intermediate between the mixed reflection asymmetric configuration and the $i_{11/2}$ shell model configuration. Comparison of the systematics of ^{219}Rn with neighboring isotones, isobars, and isotopes shows clearly the collapse of the quadrupole-octupole-type configurations into the less degenerate shell model configurations. [S0556-2813(98)02901-X]

PACS number(s): 21.60.Cs, 23.20.Lv, 23.60.+e, 27.80.+w

I. INTRODUCTION

The nucleus $^{219}Rn_{133}$ lies in a strategic transition region of the nuclear periodic table on the edge of the light actinide region which is known to involve intrinsic reflection asymmetry and corresponding unique spectroscopic features. These include parity doublet bands connected by enhanced $E1$ transitions which result from parity mixed Nilsson orbitals. On the other hand, it has only 7 neutrons beyond the 126 closed neutron shell, and might be expected to show some residual effects from shell model neutron orbitals such as $g_{9/2}$, $i_{11/2}$, and $j_{15/2}$. Indeed the ^{219}Rn ground state decays to the ^{215}Po $9/2^+$ [$g_{9/2}$ ground state with the fairly low alpha decay hindrance factor (HF) of 11 [1]] which implies a close relationship between these two ground states.

Furthermore, ^{219}Rn is of special interest because of the possibility of comparing it with the reasonably well-studied isobars ^{219}Fr and ^{219}Ra with the isotones ^{221}Ra and ^{223}Th and with the isotope ^{217}Rn.

II. PREVIOUS EXPERIMENTAL WORK

The early very careful experimental work [2] of ^{223}Ra alpha decay using a magnetic spectrograph led to a network of ^{219}Rn levels on which later work has been based. Gamma-ray studies, alpha-gamma coincidence, various types of angular correlations, and internal conversion research from a large number of different authors [3–9] have led to a fairly extensive level scheme. However, the uncertainties in spins have made interpretation very difficult and uncertain.

Since the interpretations [1–8] of the ^{219}Rn spin parities, a very significant finding—that the ^{223}Ra ground state has spin parity $3/2^+$, not $1/2^+$ [10]—influences considerably the determination of different spins. For example, the alpha decay HF to the 269 keV state, the lowest observed in ^{219}Rn at 4.7 [1] or 4.5 in Nuclear Data Tables [11], appears to imply a definite $3/2^+$ spin parity assignment for this state. Furthermore, all alpha-decay–gamma angular coincidence data should be reinterpreted. In this paper, then, we investigate again the levels in ^{219}Rn using the alpha decay of ^{223}Ra and the resulting coincident gamma rays. Two additional levels, more than 20 additional gamma transitions, and in particular a reinterpretation of the lowest levels in ^{219}Rn, have led to a much more complete understanding.

III. EXPERIMENTAL METHODS AND RESULTS

The ^{223}Ra source was obtained from ^{227}Ac with which it was in secular equilibrium. The ^{227}Ac activity was purchased several years ago from the Radiochemical Center, Amersham, England, and continues to be useful because of its 21.8 yr half-life. The ^{223}Ra is separated from the ^{227}Ac activity by heating it to 1600 °C and collecting on a thin (30 μm) Al

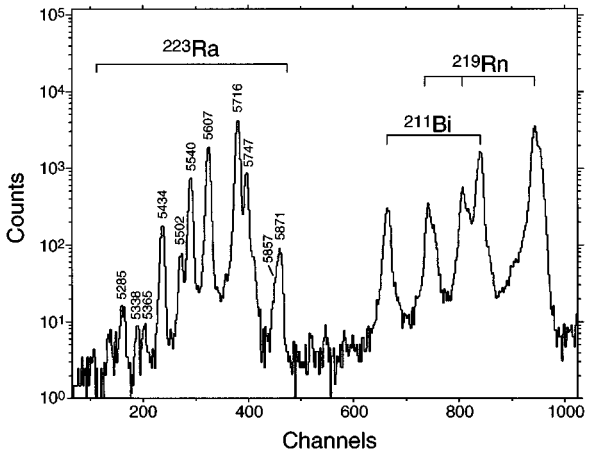

FIG. 1. The alpha spectra of ^{223}Ra, ^{219}Rn, and ^{211}Bi. Alphas from the various activities are bracketed. Alphas from ^{223}Ra leading to levels in ^{219}Rn are labeled with their energies in keV.

*Electronic address: sheline@nucmar.physics.fsu.edu

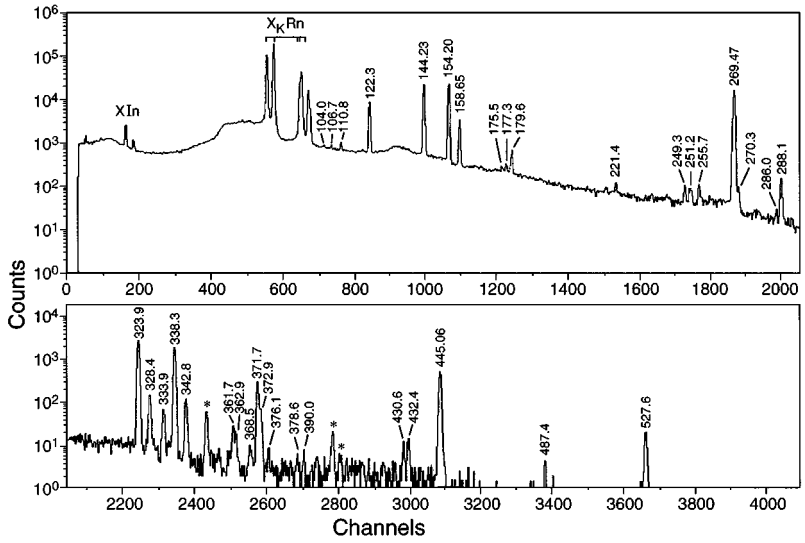

FIG. 2. Gamma spectra of ^{219}Rn in coincidence with all ^{223}Ra alphas in Fig. 1 taken with a high resolution planar Ge detector. Energies of the ^{219}Rn gammas are indicated in keV. Daughter activities are indicated with asterisks.

foil. While the ^{223}Ra evaporates at this temperature, producing a uniform thin source, the ^{227}Ac and ^{227}Th will not begin significant evaporation until ~1900 °C. Almost immediately after the evaporation, the source of ^{223}Ra is in secular equilibrium with ^{219}Rn (4.0 s) and ^{215}Po (1.78 ms). Within a few hours it is also in secular equilibrium with ^{211}Pb (36.1 m), ^{211}Bi (2.15 m), and ^{211}Po (0.52 s).

The sources were used in α-γ high resolution coincidence with a planar Ge gamma detector and also with a high efficiency 20% coaxial Ge gamma detector. Simple alpha and gamma spectra and 256 channel×4000 channel alpha-gamma coincidence measurements were recorded simultaneously over a period of 5 days.

One example of the alpha spectrum of ^{223}Ra and some of its daughters is shown in Fig. 1. Major peaks in the ^{223}Ra alpha spectrum are labeled in keV, whereas daughter alpha groups are bracketed and labeled. The planar gamma spectrum coincident with all ^{223}Ra alphas in Fig. 1 is given in Fig. 2. Gamma rays are labeled in keV and K x rays of Rn indicated. Three sets of gamma ray doublets are clearly observed at 269.5 and 270.3, 361.7 and 362.9, and 371.7 and 372.9 keV. Asterisks indicate gamma rays arising from daughter activities. Figure 3 is a composite of coaxial gamma spectra coincident with very weak alpha groups leading to the high energy part of the ^{219}Rn level scheme with specific emphasis on new levels and new transitions.

Finally, Table I lists all ^{219}Rn gamma rays observed in these experiments, their energies, intensities, multipolarities (when available), and assignment in the level scheme.

IV. LEVEL SCHEME OF ^{219}Rn

The level scheme of ^{219}Rn below 733 keV is given in Fig. 4. It is limited to the levels and, to the right, their energies in keV. Also to the extreme right the energies of the populating alphas in keV, their intensities, and their hindrance factors (HF's) are given [2,19]. Transitions are shown as vertical lines with their energies in keV. A second simplified level scheme emphasizing spin parities and configurational assignments is given in Sec. V.

The level structure as distinct from the spin assignments is clearly established and only slightly different from that of previous authors [1,11] up to 446.7 keV. These differences include the replacement of the 378.5 keV level with a 377.3 keV level with different decay properties and a new 490.8 keV level not populated in alpha decay, but observed through gamma population and depopulation. The level structure is based on the magnetic spectrograph data [2], slightly refined [8,19]. Our high resolution and high statistics alpha-gamma coincidences allow us to construct the level scheme and put more than 20 new transitions firmly in the decay scheme. We then proceed to the more difficult task of assigning spins, parities, and, if possible, configurations to the level.

A. Spin assignments in ^{219}Rn

The ground state of ^{219}Rn has previously [1,11] been given the J^{π} assignment of $5/2^{+}$. Its 5/2 spin has been un-

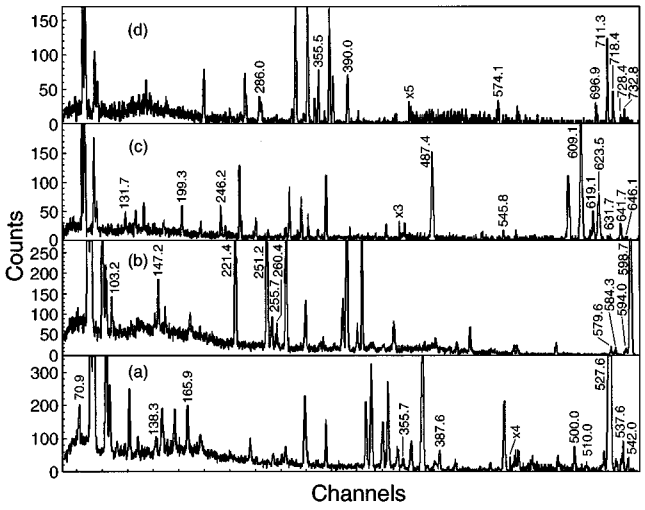

FIG. 3. Gamma spectra of ^{219}Rn in coincidence with various weak alpha groups of ^{223}Rn as observed with a coaxial Ge detector. (a) Coincidences with the 5366 and 5339 keV alpha groups, (b) with the 5287 and 5283 keV alpha groups, (c) with the 5259 and 5236 and 5212 keV alpha groups, and (d) with the 5713 and 5152 keV alpha groups. Gamma energies are given in keV. Note that energy calibrations are different for each of the panels and also the counting rate scale factors.

TABLE I. Gamma ray transitions in ^{219}Rn following the alpha decay of ^{223}Ra.

$E_\gamma(\Delta E)$	I_γ[a]	Multipolarity[b]	Level Initial→Final	$E_\gamma(\Delta E)$	I_γ[a]	Multipolarity[b]	Level Initial→Final
4.4 (1)			4.4 →0	342.80(7)	1.6 (1)	$E1$	342.8→0
10.0 (1)			14.4 →4.4	355.5 (2)[c]	0.03 (1)		732.8→377.3
14.4 (1)			14.4 →0	355.7 (2)[c]	0.02 (1)		514.4→158.7
31.9 (1)	0.001	$E2$	158.7 →126.8	361.7 (1)	0.20 (5)		376.1→14.4
34.5 (2)[c]			377.3 →342.8	362.9 (2)[c]	0.11 (5)		377.3→14.4
69.5 (1)[c]	0.05 (2)	$M1$	446.8 →377.3	368.5 (1)	0.06 (3)		711.3→342.8
70.9 (2)[c]	0.025 (8)		(517.7)→446.8	371.7 (1)	3.5 (1)	$M1+E2$	376.1→4.4
102.2 (2)[c]	0.006 (3)		445.0 →342.8	372.9 (1)[c]	0.36	$E1$	377.3→4.4
103.2 (2)[c]	0.04 (2)	$E2+M1$	594.0 →490.8	376.1 (2)	0.09 (3)		376.1→0
104.0 (2)	0.14 (2)	$M1+E2$	446.8 →342.8	387.6 (2)	0.11 (4)		514.4→126.8
106.7 (1)	0.17 (1)	$M1$	445.0 →338.3	390.0 (2)	0.05 (2)		732.8→342.8
108.5 (2)[c]	0.04 (2)		446.8 →338.3	430.6 (3)	0.14 (4)		445.0→14.4
110.8 (1)	0.42 (3)	$E2$	269.5 →158.7	432.4 (3)	0.25 (2)		446.8→14.4
(112.6)			711.3 →598.7	445.06 (5)	9.3 (3)	$M1$	445.0→0
114.7 (2)	0.07 (3)		490.8 →376.1	487.4 (2)	0.08 (1)		646.1→158.7
122.32 (7)	8.7 (1)	$M1$	126.8 →4.4	490.8 (3)[c]	0.012 (5)		
131.7 (2)	0.04 (2)		646.1 →514.4	500.0 (4)[c]	0.010 (4)		514.4→14.4
138.3 (3)[c]	0.012 (5)		514.4 →376.1	510.0 (4)[c]	0.003 (2)		514.4→4.4
144.23 (3)	23.5 (5)	$M1+E2$	158.7 →14.4	523.2 (4)[c]	0.010 (4)		
147.2 (2)[c]	0.04 (2)		594.0 →446.8	527.6 (1)	0.51 (3)		542.0→14.4
154.20 (3)	41 (1)	$M1+E2$	158.7 →4.4	532.9 (4)[c]	0.010 (4)		
158.65 (5)	5.0 (1)	$M1+E2$	158.7 →0	537.6 (1)[c]	0.015 (5)		542.0→4.4
165.9 (2)	0.04 (2)		542.0 →376.1	542.0 (4)[c]	0.010 (4)		542.0→0
175.5 (2)	0.14 (3)		445.0 →269.5	545.8 (5)[c]	0.008 (4)		672.6→126.8
177.3 (1)	0.34 (3)		446.8 →269.5	574.1 (7)[c]	0.008 (4)		732.8→158.7
179.6 (1)	1.1 (1)	$M1+E2$	338.3 →158.7	579.6 (3)[c]	0.010 (4)		594.0→14.4
199.3 (3)	0.02 (1)		646.1 →446.8	584.3 (3)[c]	0.010 (4)		598.7→14.4
221.4 (1)	0.26 (4)	$E1$	598.7 →377.3	594.0 (3)[c]	0.010 (4)		594.0→0
246.2 (3)	0.07 (2)		623.5 →377.3	598.7 (1)	0.68 (3)		598.7→0
249.3 (1)	0.28 (7)	$M1+E2$	376.1 →126.8	609.1 (1)	0.41 (2)		623.5→14.4
251.2. (2)	0.3 (1)	$M1+E2$	594.0 →342.8	619.1 (4)[c]	0.025 (8)		623.5→4.4
255.1 (2)	0.38 (5)		269.5 →14.4	623.5 (3)	0.06 (3)		623.5→0
255.7 (3)	0.04 (2)		594.0 →338.3	631.7 (7)	0.003 (2)		646.1→14.4
260.4 (3)	0.05 (2)		598.7 →338.3	641.7 (4)[c]	0.012 (5)		646.1→4.4
269.47 (3)	100 (2)	$M1$	269.5 →0	646.1 (5)[c]	0.003 (3)		646.1→0
270.3 (4)[c]	0.005 (3)		397.1 →126.8	696.9 (7)[c]	0.005 (2)		711.3→14.4
286.0 (4)[c]	0.008 (4)		732.8 →446.8	711.3 (2)	0.026 (7)		711.3→0
288.1 (1)	1.15 (3)	$E1$	446.8 →158.7	718.4 (4)[c]	0.010 (4)		732.8→14.4
323.90 (5)	28.7 (5)	$M1+E2$	338.3 →14.4	728.4 (8)[c]	0.002 (1)		732.8→4.4
328.4 (1)	1.5 (5)	$E1$	342.8 →14.4	732.8 (6)[c]	0.004 (2)		732.8→0
333.9 (1)	0.73 (4)	$E2$	338.3 →4.4	737.2 (8)[c]	0.002 (1)		
338.32 (5)	20.4 (4)	$M1+E2$	338.3 →0				

[a]Gamma intensities normalized with previous data [1].
[b]Multipolarities from magnetic conversion electron measurements [8].
[c]New gamma-ray transitions observed.

ambiguously determined by collinear fast beam laser spectroscopy [12] and the positive parity strongly implied by the low HF [11] of the ^{219}Rn→^{215}Po alpha decay. As mentioned in Sec. II, the 269.5 keV state can be assigned a definite spin parity of $3/2^+$ because of the low HF populating it from the ^{223}Ra $3/2^+$ ground state. It decays to the $5/2^+$ ground state as expected, with a mixed $M1+E2$ gamma ray. The $3/2^+$ state at 269.5 keV also decays to the 158.7 keV state with a

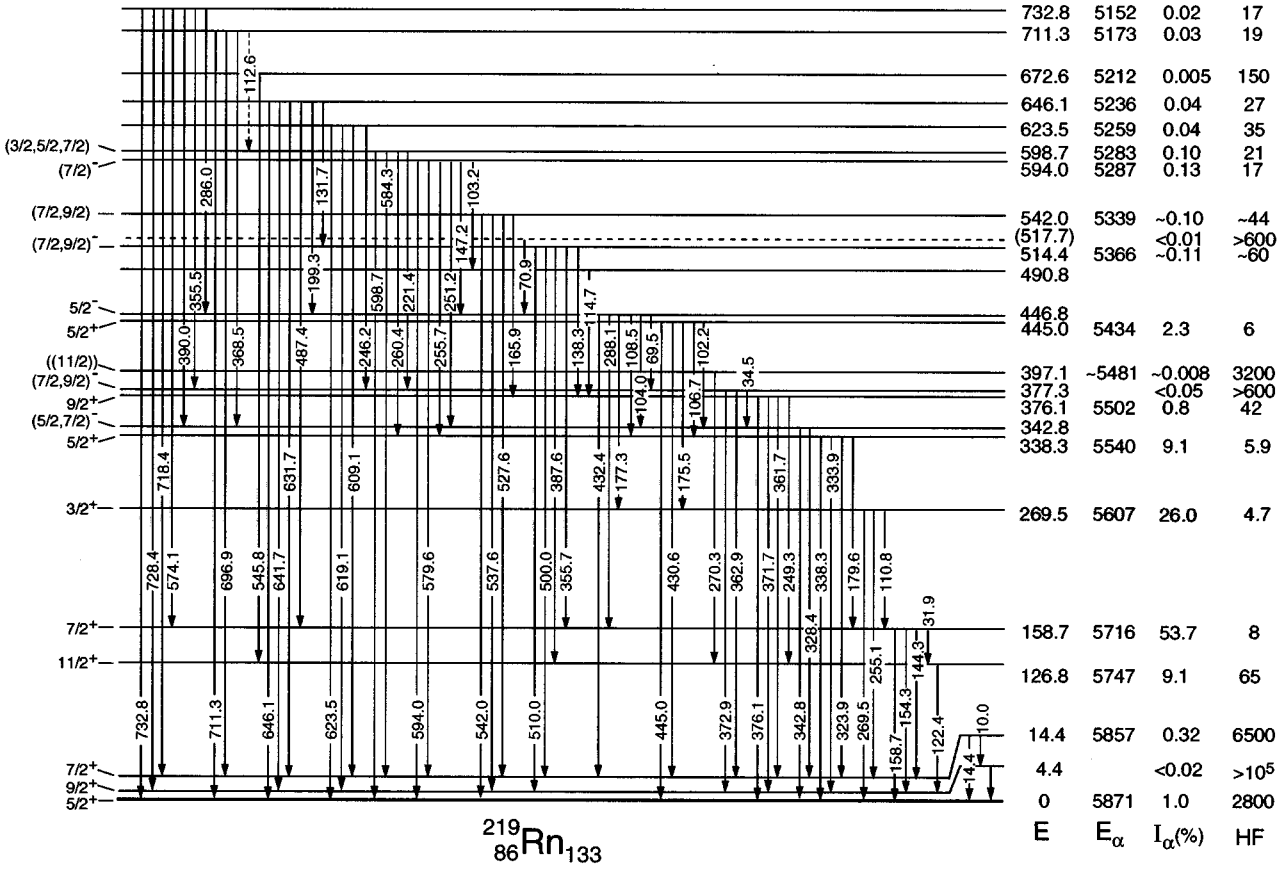

FIG. 4. Energy level scheme of ^{219}Rn up to 733 keV resulting from the present study. Alpha energies in keV, their intensities and hindrance factors (HF's) populating the levels are shown to the right and are taken from magnetic spectrograph measurements [2,19]. Transitions are shown as vertical lines with their energies in keV. Spins, parities, and configurations are shown in the simplified level scheme of Fig. 5.

collective pure $E2$ transition whose $B(E2)$ is 69 Weisskopf units (W.u.) [10], strongly suggesting $J^{\pi}=7/2^{+}$. The $7/2^{+}$ 158.7 keV state decays by a collective $E2$ transition to a state at 126.8 keV. Since the 126.8 keV state is not populated by the 269.5 keV $3/2^{+}$ state and does not decay to the $5/2^{+}$ ground state, we suggest spin parity $11/2^{+}$.

The very low lying level structure of ^{219}Rn is unusual in that there are three states within the first 15 keV. The 4.46 and 14.38 keV states have each had multiple spin-parity assignments [1,11]. However, we note that the 158.7 keV $7/2^{+}$ state and the 126.8 keV $11/2^{+}$ state both decay to the 4.46 keV state with mixed $M1+E2$ transitions, fixing $9/2^{+}$ as the spin of the 4.46 keV state. The only difficulty is that the internal conversion spectrum of the 4.46 keV transition to the ground state $5/2^{+}$ has been measured as mixed $M1+E2$ [9] instead of $E2$. This multipolarity assignment is based on the ratio of N_1 to N_2 to N_3 conversion electron intensities [9]. However, the very weak N_1 intensity is very dependent on how the strong N_2 and N_3 tails are drawn. We note that the expected ratio $N_1/N_2/N_3$ of 1/85/109 for a pure $E2$ transition [13] is equally in agreement with the data [9]. Therefore we believe the 4.46 keV transition is $E2$ and the spin of the 4.46 keV state, $9/2^{+}$. Once this assumption is made, the integrity of the entire set of spin parities of ^{219}Rn is obvious. This is perhaps the most significant reason for assigning $9/2^{+}$ to the 4.46 keV state. It follows then directly that the 14.38 keV state which decays to the $9/2^{+}$ 4.46 keV and $5/2^{+}$ ground state with mixed $M1+E2$ transitions must be $7/2^{+}$.

Having established the spin parities of the lowest six states with a range of spins from 3/2 to 11/2, it is then often possible to determine unique spins and parities for the states which lie higher in energy. For example, the next state at 338.3 keV decays by $M1$ or $M1+E2$ to the $5/2^{+}$ ground state, the $7/2^{+}$ 14.4 keV state, and the $7/2^{+}$ 158.7 keV state and by $E2$ to the $9/2^{+}$ 4.4 keV state, fixing its spin parity as $5/2^{+}$. In some cases only multiple spin assignments are possible, as, for example, for the 342.8 keV state where $5/2^{-}$ and $7/2^{-}$ are possible. For model reasons we prefer the $5/2^{-}$ assignment. Spins of higher lying levels follow from the populating and depopulating transitions. We will mention only those instances in which there is a discrepancy with the accepted level scheme [1,11]. A level at 378.5 keV has been proposed [1,11] with one depopulating transition. We find no evidence for this level or transition. We do find evidence for a new 377.3 keV level (not populated by alpha decay) with three depopulating transitions which define spin parity $7/2^{-}$ or $9/2^{-}$. We also find evidence for a 490.8 keV level (not previously observed) which is depopulated by a 114.7 keV $M1$ transition to the 376.1 keV transition. In view of the additional spins and parities proposed in this research and the

TABLE II. Comparison of the experimental and theoretical angular correlation coefficients $[A_2(\alpha,\gamma)]$ for the alpha decay of ^{223}Ra to the 158.7 keV state in ^{219}Rn and its subsequent gamma decay to the ^{219}Rn ground state and 4.4 and 14.4 keV states.

			$A_2(\alpha,\gamma)$ (calc.)	
E_γ	Gamma transition	$A_2(\alpha,\gamma)$ (expt.)	$\delta<0$	$\delta>0$
144.3	7/2→7/2	$+(0.37\pm0.04)$	$+(0.34\pm0.02)$	$-(0.52\pm0.02)$
154.3	7/2→9/2	$-(0.07\pm0.02)$	$-(0.06\pm0.04)$	$+(0.26\pm0.04)$
158.7	7/2→5/2	$+(0.11\pm0.03)$	$+(0.10\pm0.07)$	$+(0.71\pm0.07)$

newly established $3/2^+$ ground state spin of ^{223}Ra, it is especially important to reinterpret angular correlation results.

B. Interpretation of alpha-gamma angular correlation

There have been numerous alpha-gamma angular correlation studies of ^{223}Ra alpha decay [5,6,9] including one from our laboratory [8].

We can now reinterpret the alpha-gamma angular correlation results with much more confidence using the known ^{223}Ra and ^{219}Rn ground state spins of 3/2 and 5/2, respectively, from collinear laser spectroscopy [10,12].

The anisotropy coefficients A_2 and A_4 of α-$\gamma(\theta)$ are composed of two terms:

$$A_n(\alpha,\gamma)=A_n(\alpha)*A_n(\gamma), \tag{1}$$

where

$$A_n(\alpha)=[F_n^\alpha(I_iILL)+2\Delta F_n^\alpha(I_iILL') + \Delta^2 F_n^\alpha(I_iIL'L')]/(1+\Delta^2), \tag{2}$$

$$A_n(\gamma)=[F_n^\gamma(I_fIll)+2\delta F_n^\gamma(I_fIll') + \delta^2 F_n^\gamma(I_fIl'l')]/(1+\delta^2). \tag{3}$$

I_i, I, and I_f are spin values of the initial, intermediate, and final states; Δ^2 and δ^2, are angular momentum mixing (L,L') for alpha and (l,l') for gamma transitions.

The 158.7 keV level of ^{219}Rn is a particularly interesting case. This level is strongly populated by alpha decay and there are three intense gamma 144.3, 154.3, and 158.7 keV depopulating transitions decaying to 14.4, 4.4, and the ground state of ^{219}Rn. Their $E2/M1$ mixing is well established by magnetic electron conversion measurements [8]:

144.3 keV $M1+(1.5\pm0.5)\%$ $E2$,
154.3 keV $M1+(0.6\pm0.3)\%$ $E2$,
158.7 keV $M1+(5.0\pm1.5)\%$ $E2$.

We have proposed the spin $7/2^+$ for the 158.7 keV intermediate state. For an alpha decay of $3/2^+$ to $7/2^+$ ($L=2$, $\Delta^2\simeq0$) the $A_2(\alpha)$ is -0.95.

Using the spins 5/2, 9/2, 7/2, and 7/2 for the ground state, 4.4, 14.4, and 158.7 keV states of ^{219}Rn and $A_2(\alpha)=-0.95$ we have calculated the angular correlation coefficients $[A_2(\alpha,\gamma)]$ and compared them with experiment. The results are summarized in Table II.

We find a very nice agreement between the $A_2(\alpha,\gamma)$ experimental values and the calculated values if the gamma mixing phase is negative. These results reinforce our proposed spins 9/2 for the 4.4, 7/2 for the 14.4 and 158.7 keV levels.

V. DISCUSSION

One feature of the level scheme of ^{219}Rn (Fig. 4) is immediately evident. There are two groups of alphas, with very different HF's. To emphasize this point and others involving the configurations a simplified level scheme is presented in Fig. 5 in which all of the gamma transitions have been removed and levels with similar HF's have been grouped together. The high HF's range from 2400 to $>10^5$ and the corresponding alphas populate the first three states all of which lie below 15 keV. The rest of the states in this group, except the 397 keV state (HF 3100) which is shown to the left in Fig. 5, are not populated in alpha decay, implying very high HF's. On the other hand, the rest of the states shown in the right two columns of Fig. 5 have much lower HF's which range from 4.5 to 65.

A second fairly obvious feature is that the lowest negative parity state of the states populated with high alpha decay HF's lies $\sim$340 keV above the lowest positive parity state, while among the states populated with low HF's the difference is $\sim$320 keV. Both of these features of the ^{219}Rn level scheme may be understood in terms of the underlying configurations.

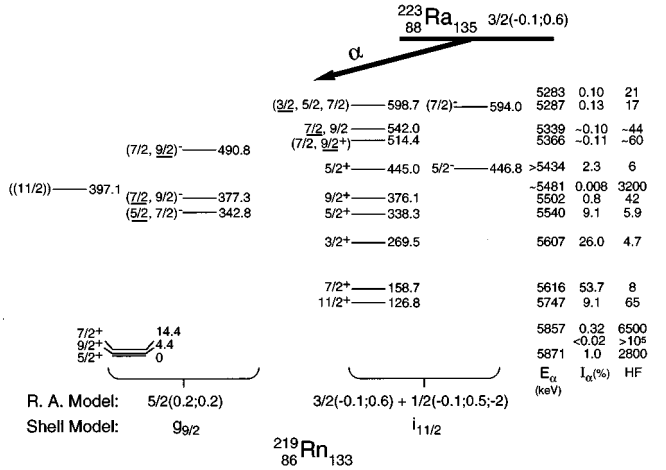

FIG. 5. Schematic level scheme of ^{219}Rn showing spins, parities, and configurations. Where multiple spin assignments are given, the underlined spin is most consistent with the reflection asymmetric model.

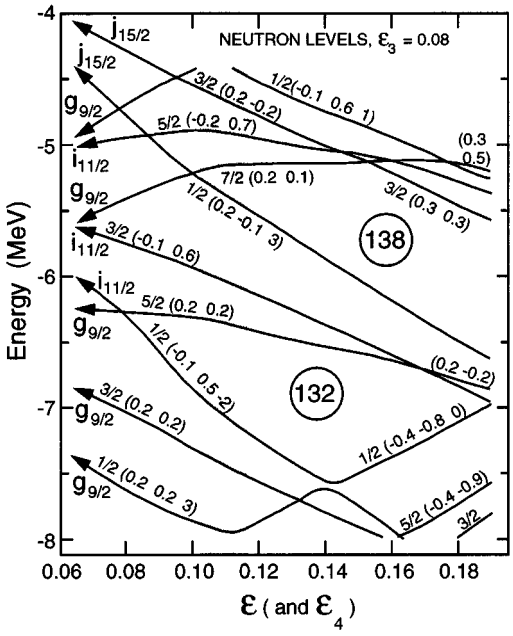

FIG. 6. Parity mixed neutron orbitals calculated in an axially symmetric but reflection asymmetric ($\epsilon_3 = 0.08$) folded Yukawa potential [14] plotted against quadrupole deformation (ϵ). The orbitals are labeled by Ω and in parentheses by single particle matrix elements $\langle \hat{s}_z \rangle$, $\langle \hat{\pi} \rangle$, and if $\Omega = 1/2$, also $\langle \pi_{\text{conj}} | -\hat{J}_+ | R_{\text{conj}} \rangle$.

A. Configurations in ^{219}Rn

Figure 6 presents the octupole deformed Nilsson orbitals calculated with an axially symmetric reflection asymmetric folded Yukawa potential [14]. The levels are labeled by $\Omega(\langle \hat{s}_z \rangle, \langle \hat{\pi} \rangle)$, and in the case of $K = 1/2$ orbitals, a third quantum number listed last in the parentheses $\langle \pi_{\text{conj}} | -\hat{J}_+ | R_{\text{conj}} \rangle$. These are parity mixed orbitals so that each orbital gives rise to two bands with positive and negative parity. In the most strongly octupole deformed nuclei, the two bands lie fairly close in energy.

The ground state of the alpha decaying parent, 135 neutron ^{223}Ra, should have configuration $3/2(-0.1, 0.6)$ at quadrupole deformation $\epsilon \sim 0.12$ according to Fig. 6. One observes [15] a $K = 3/2^+$ ground state rotational band and ~ 50 keV above the parity doublet $K = 3/2^-$ band as predicted in ^{223}Ra. On the other hand, the 133 neutron ^{219}Rn daughter of ^{223}Ra should have a ground state configuration $5/2(0.2, 0.2)$ and a first excited state configuration $3/2(-0.1, 0.6)$, the same as the ground state of ^{223}Ra.

In the level scheme (Fig. 5) of ^{219}Rn we note that the ground state does have spin parity $5/2^+$. However, the structure $5/2^+$, $9/2^+$, $7/2^+$ all within 15 keV is very curious, and is an indication of the transitional nature of the ^{219}Rn levels. As we shall see, however, by a comparison with other $K = 5/2^+$ bands in this region, the level structure is understandable in terms of the overall systematics. It should also be noted that very high alpha decay HF's are expected for the $5/2(0.2, 0.2)$ configuration since the parent has the configuration $3/2(-0.1, 0.6)$. These two configurations at $\epsilon_3 = \epsilon = 0$ go over into the $g_{9/2}$ and $i_{11/2}$ shell model states, respectively. They are therefore quite unrelated and expected to be connected by high HF's in alpha decay.

The ^{219}Rn states populated by low HF's in alpha decay are clearly closely related to the $3/2(-0.1, 0.6)$ ^{223}Ra ground state configuration. As in the case of the $K = 5/2^+$ band, the rotational structure of the $K = 3/2^+$ band is seriously disrupted when compared with that in ^{223}Ra. It has the spin sequence $11/2^+$, $7/2^+$, $3/2^+$, $5/2^+$, $9/2^+$. Comparison of the $K = 3/2^+$ band in ^{219}Rn with that of its isotone, ^{221}Ra, shows a very similar disruption due in large part to mixing with the $K = 1/2^+$ band from the configuration $1/2(-0.1, 0.5, -2)$. This point will be made more completely in the next section with the comparison of all the $K = 3/2^+$ bands in this region.

We note the presence of negative parity bands ~ 340 and 320 keV from the positive parity bandheads. These have the appropriate spin-parity structure to be the parity doublets expected from reflection asymmetric orbitals. However, their much larger energy differences are another indication that the ^{219}Rn level structure is transitional.

Finally, it should be pointed out that the $9/2^+$ lies at only 4.4 keV and the $11/2^+$ is the bandhead of the other group of states populated with low HF's. It is clear that as the neutron number decreases toward 126, these two sets of states are going over into the $g_{9/2}$ and $i_{11/2}$ shell model states, respectively. On the basis of the above considerations, the configurations $5/2(0.2, 0.2)$ and $g_{9/2}$ are listed under one set of states in Fig. 5 while $3/2(-0.1, 0.6) + 1/2(-0.1, 0.5, -2)$ and $i_{11/2}$ are listed under the other.

B. Systematics of the band structure of the $K = 5/2^{\pm}$ bands in ^{219}Rn and in neighboring isotopes, isotones, and isobars

In order to understand the band structure of the $K = 5/2^{\pm}$ bands in ^{219}Rn, it is instructive to compare them with those of ^{223}Ra [15], with the isotone ^{221}Ra [16], with the isobar ^{219}Ra [17], and with the isotope ^{217}Rn [18]. This comparison is made in Fig. 7. All $K = 5/2^{\pm}$ bandheads in Fig. 7 (two of which begin with $J^{\pi} = 9/2^+$ states) are assigned an energy of 0 keV to put them on the same footing for the comparison. States of the same spin in the $K = 5/2^+$ bands are connected by dashed lines. Only the bandhead of the $K = 5/2^-$ band is given and is connected by dotted lines. From the left to right we go lower in mass number and towards the 126 neutron closed shell.

Toward the left hand side of Fig. 7 we see quite regular $K = 5/2^+$ bands in ^{223}Ra and ^{221}Ra which can be understood in terms of the $5/2(0.2, 0.2)$ reflection asymmetric orbital of Fig. 6. As we decrease the mass number in the isotones ^{219}Ra and ^{219}Rn, the level structure is severely compressed as a result of the sharp drop in energy of the $9/2^+$ state to become the lowest state in ^{219}Ra or very near the ground state (4.46 keV) in ^{219}Rn. At the same time the $5/2^+$ and $7/2^+$ states come much closer together. Finally, at ^{217}Rn just four protons and five neutrons away from the double closed shell in ^{208}Pb, the $9/2^+$ state has decisively become the ground state with a great deal of $g_{9/2}$ shell model character as shown by its very fast alpha decay to the $g_{9/2}$ ground state of ^{213}Po (HF$\leqslant$1.4) [1]. Meanwhile the $5/2^+$ state has crossed over the $7/2^+$ state. The trend in the $K = 5/2^+$ band in Fig. 7 is quite clear. We proceed from quite regular reflection asymmetric bands to mixed reflection asymmetric $g_{9/2}$ shell

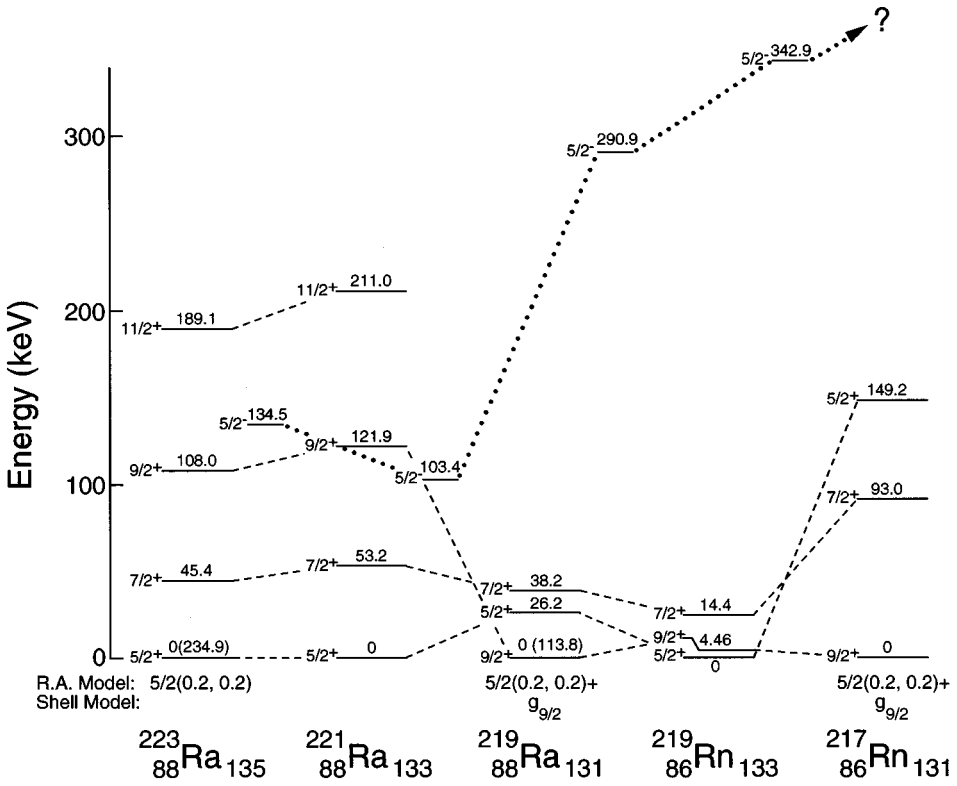

FIG. 7. Comparison of selected level structures of the $K=5/2^{\pm}$ bands of ^{223}Ra, ^{221}Ra, ^{219}Ra, ^{219}Rn, and ^{217}Rn. States of the same spin and positive parity are connected by dashed lines. States of the same spin and negative parity are connected by dotted lines. See text for interpretation.

model states with increasing dominance of the shell model character as we move toward the closed shell.

If we now look at the parity doublet $K=5/2^{-}$ bandheads in both ^{223}Ra and ^{221}Ra, they are reasonably close to their $K=5/2^{+}$ partner (103–135 keV). However, as the $g_{9/2}$ shell model character increases the $K=5/2^{-}$ shoots up sharply in energy to 291–343 keV in ^{219}Ra and ^{219}Rn, respectively. While this energy is still considerably less than that expected for the octupole vibration, it clearly indicates a lessening reflection asymmetric character. In ^{217}Rn the negative parity band has unfortunately not been observed.

C. Systematics of the band structure of the $K=3/2^{\pm}$ in ^{219}Rn and in neighboring isotopes, isotones, and isobars

The band structure of the $K=3/2^{\pm}$ bands in ^{219}Rn is compared with the same set of nuclei with which it was compared in Sec. V B. in Fig. 8. All bandheads are assigned an

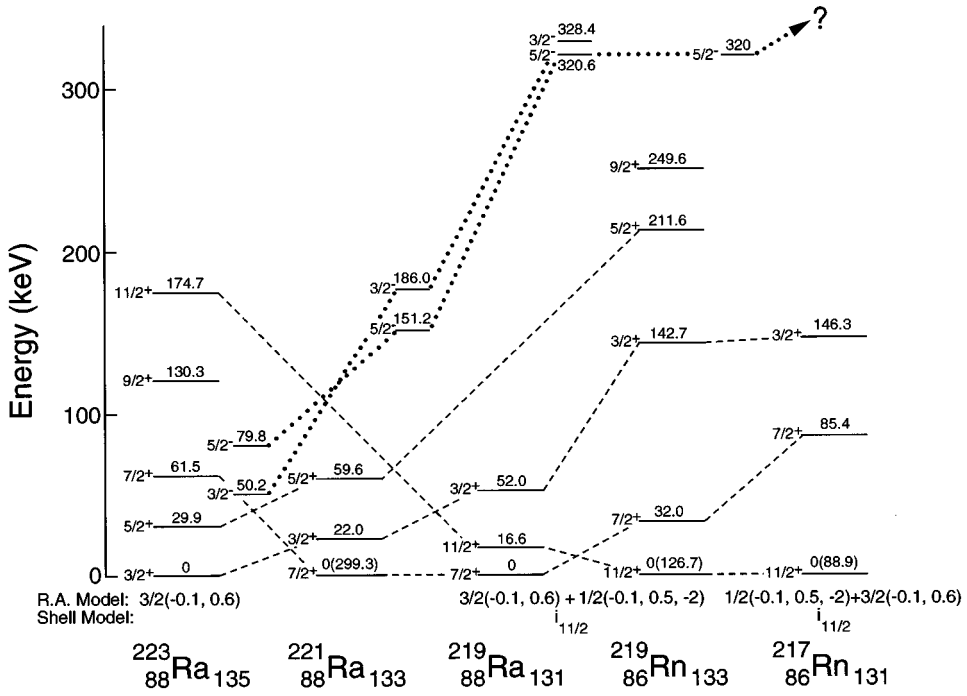

FIG. 8. Comparison of selected levels of the $K=3/2^{\pm}$ bands of ^{223}Ra, ^{221}Ra, ^{219}Ra, ^{219}Rn, and ^{217}Rn. States of the same spin and positive parity are connected by dashed lines, those of negative parity by dotted lines. See text for interpretation.

energy of 0 keV for the comparison. States of the same spin in the $K=3/2^+$ bands are connected by dashed lines while the $3/2^-$ and $5/2^-$ states of the $K=3/2^-$ bands are connected by dotted lines. The ordering of the nuclei in Fig. 8 is the same as that in Fig. 7. From the left we move in decreasing mass number toward the 126 neutron closed shell, with the three Ra nuclei, ^{223}Ra, ^{221}Ra, and ^{219}Ra, followed by the two Rn nuclei ^{219}Rn and ^{217}Rn.

At the extreme left of Fig. 8, the $K=3/2^+$ band of ^{223}Ra has a reasonably regular rotational structure, although there is evidence that the states of negative simplex quantum number (i.e., $3/2^+$, $7/2^+$, and $11/2^+$) are lowered with respect to states with positive simplex quantum number ($5/2^+$, $9/2^+$). By the time we reach ^{221}Ra in the systematics, the $7/2^+$ state has become the bandhead. It remains the bandhead in ^{219}Ra. However, in ^{219}Ra the $11/2^+$ state has come down all the way to 16.6 keV. In ^{219}Rn the $11/2^+$ state is the bandhead and becomes even more decisively so in ^{217}Rn.

The fact that the negative simplex states move down in energy in the $K=3/2^+$ bands results from two effects. The first is the Coriolis coupling of the $K=3/2^+$, $3/2(-0.1,\ 0.6)$ band with the $K=1/2^+$, $1/2(-0.1,\ 0.5,\ -2)$ band. Figure 6 indicates for 133 neutron nuclei at $\epsilon\sim 0.10$ the first excited configuration should be $3/2(-0.1,\ 0.6)$. However, the hole configuration $1/2(-0.1,\ 0.5,\ -2)$ should occur nearby probably higher in energy. With a large negative decoupling parameter it will push down the negative simplex states.

The second effect on the systematics is the approach toward spherical symmetry and the $i_{11/2}$ shell model state. These two effects reinforce each other. For example, as we approach spherical symmetry the energy difference between the 1/2 and 3/2 band decreases, the Coriolis coupling constant increases and the negative decoupling parameter of the $K=1/2$ band becomes more negative. All of these effects cause the negative simplex states to move down in energy until the normal band structure is destroyed and the $11/2^+$ state becomes the bandhead and finally the $i_{11/2}$ shell model state. These effects are obvious in Fig. 8.

At the same time the $K=3/2^-$ parity doublet partner increases in energy from 50 keV in ^{223}Ra to 320 keV in ^{219}Ra and ^{219}Rn. In fact, the energy splitting in the $K=5/2^\pm$ and $K=3/2^\pm$ parity doublet bands is remarkably similar in ^{219}Ra and ^{219}Rn. This suggests that the octupole collectivity is decreasing. It is also interesting that just as the negative simplex states are lowered for the $3/2^+$ band, the positive simplex states are lowered for the $3/2^-$ parity doublet band. This is indicated in Fig. 8 by the reversal in order of the $3/2^-$ and $5/2^-$ states in ^{221}Ra and ^{219}Ra and is expected since the parity doublet $1/2^-$ band will have positive decoupling parameters.

VI. CONCLUSIONS

The level structure of ^{219}Rn has been studied using the alpha decay of ^{223}Ra together with the coincident gamma rays. The level scheme resulting from the synthesis of previous data [1,11] up through the 342.8 keV level, insofar as levels and transitions are concerned, is confirmed. Above this energy some changes in the level structure and additional transitions are required.

Quite different spins and parities are required for many levels previously assigned. In addition, many new spin-parity assignments have been proposed.

Using reflection asymmetric Nilsson orbitals the alpha decaying ground state of ^{223}Ra is known to have configuration $3/2(-0.1,\ 0.6)$. It decays to excited states in ^{219}Rn with low HF's and the same configuration. The ground state of ^{219}Rn and a few higher energy states populated with much higher HF's in alpha decay are shown to have configuration $5/2(0.2,\ 0.2)$. However, the band structures of both $K=3/2^\pm$ and $5/2^\pm$ bands are very anomalous. In order to sort out the band structures, the systematics of the bands arising from the configurations $5/2(0.2,\ 0.2)$ and $3/2(-0.1,\ 0.6)$ is studied in ^{223}Ra, ^{221}Ra, ^{219}Ra, ^{219}Rn, and ^{217}Rn. In this way it is possible to understand the anomalies in the band structures and to interpret the $K=5/2^\pm$ bands as intermediate between the $5/2(0.2,\ 0.2)$ reflection asymmetric configuration and the $g_{9/2}$ shell model configuration. In a similar way the $K=3/2^\pm$ bands are interpreted as intermediate between the mixed $3/2(-0.1,\ 0.6)+1/2(-0.1,\ 0.5,\ -2)$ reflection asymmetric configurations and the $i_{11/2}$ shell model configuration.

One of us (R.K.S.) wishes to thank the National Science Foundation for support under Contract No. PHY92-07336 with Florida State University, and for the hospitality of the CSNSM and the IPN at the Université de Paris-Sud, Campus Orsay.

[1] C. M. Lederer and V. S. Shirley, *Table of Isotopes*, 7th ed. (Wiley, New York, 1978).
[2] R. J. Walen, V. Nedovesov, and G. Bastin-Scoffier, Nucl. Phys. **35**, 232 (1962).
[3] C. Briançon, C. F. Leang, and R. Walen, C. R. Seances Acad. Sci., Ser. B **266**, 1533 (1968).
[4] D. Bertault, M. Vidal, and G. Y. Petit, J. Phys. (Paris) **30**, 909 (1969).
[5] K. Krien, C. Gunther, J. D. Bowman, and B. Klemme, Nucl. Phys. **A141**, 75 (1970).
[6] W. F. Davidson and R. D. Connor, Nucl. Phys. **A149**, 363 (1970).
[7] W. H. A. Hesselink, Ph.D. thesis, University of Delft, 1972.
[8] N. T. Phuoc, Ph.D. thesis, University of Paris (Sud), 1972.
[9] B. Richter, M. J. Canty, L. Ley, M. V. Banaschik, and A. Neskakis, Nucl. Phys. **A223**, 234 (1974).
[10] S. A. Ahmad, W. Klempt, R. Neugart, E. W. Otten, K. Wendt, and C. Ekström, Phys. Lett. **133B**, 47 (1983).
[11] E. Browne, Nucl. Data Sheets **65**, 669 (1992).
[12] W. Borchers, R. Neugart, E. W. Otten, H. T. Duong, G. Ulm, K. Wendt, and the Isolde Collaboration, Hyperfine Interact. **34**, 25 (1987).
[13] H. Rösel, H. M. Fries, K. Alder, and H. C. Pauli, At. Data Nucl. Data Tables **21**, 291 (1978).

[14] G. A. Leander and R. K. Sheline, Nucl. Phys. **A413**, 375 (1984).
[15] R. K. Sheline, Phys. Lett. **166B**, 269 (1986); R. K. Sheline, G. A. Leander, and Y. S. Chen, Nucl. Phys. **A486**, 306 (1988).
[16] C. F. Liang, P. Paris, Ch. Briançon, and R. K. Sheline, Int. J. Mod. Phys. A **5**, 1551 (1990).
[17] R. K. Sheline, C. F. Liang, and P. Paris, Czech. J. Phys. **43**, 603 (1993).
[18] C. F. Liang, P. Paris, and R. K. Sheline, Phys. Rev. C **55**, 2768 (1997).
[19] A. Rytz, At. Data Nucl. Data Tables **47**, 205 (1991).